

Nucleon Polarizabilities from Low-Energy Compton Scattering

S.R. Beane¹, M. Malheiro², J.A. McGovern³, D.R. Phillips^{1,4}, and U. van Kolck^{5,6}

¹Department of Physics, University of Washington, Seattle, WA 98195-1560, USA

²Instituto de Física, Universidade Federal Fluminense, 24210-340, Niterói, R.J., Brazil

³Department of Physics and Astronomy, University of Manchester, Manchester M13 9PL, UK

⁴Department of Physics and Astronomy, Ohio University, Athens, OH 45701, USA

⁵Department of Physics, University of Arizona, Tucson, AZ 85721, USA and

⁶RIKEN BNL Research Center, Brookhaven National Laboratory, Upton, NY 11973, USA

An effective field theory is used to give a model-independent description of Compton scattering at energies comparable to the pion mass. The amplitudes for scattering on the proton and the deuteron, calculated to fourth order in small momenta in chiral perturbation theory, contain four undetermined parameters that are in one-to-one correspondence with the nucleon polarizabilities. These polarizabilities are extracted from fits to data on elastic photon scattering on hydrogen and deuterium. For the proton we find: $\alpha_p = (12.1 \pm 1.1)^{+0.5}_{-0.5} \times 10^{-4} \text{ fm}^3$, $\beta_p = (3.4 \pm 1.1)^{+0.1}_{-0.1} \times 10^{-4} \text{ fm}^3$. For the isoscalar polarizabilities we obtain: $\alpha_N = (9.0 \pm 1.5)^{+3.6}_{-0.8} \times 10^{-4} \text{ fm}^3$, $\beta_N = (1.7 \pm 1.5)^{+1.4}_{-0.6} \times 10^{-4} \text{ fm}^3$.

Electromagnetic polarizabilities are a fundamental property of any composite object. For example, atomic polarizabilities contain information about the charge and current distributions that result from the interactions of the protons, neutrons, and electrons inside the atom. Protons and neutrons are, in turn, complex objects composed of quarks and gluons, with interactions governed by QCD. It has long been hoped that neutron and proton polarizabilities will give important information about the strong-interaction dynamics of QCD. For example, in a simple quark-model picture these polarizabilities contain averaged information about the charge and current distribution produced by the quarks inside the nucleons [1]. In this paper we use an effective field theory (EFT) of QCD to extract *nucleon* polarizabilities in a consistent and systematic manner from Compton scattering data—the first EFT extraction of these important quantities.

In an atomic or molecular system the polarizabilities are measured with static fields. Nuclear polarizabilities can analogously be determined by the scattering of long-wavelength photons. Experimental facilities which accurately measure the energy of a photon beam using photon tagging have made possible a new generation of experiments which probe the low-energy structure of nucleons and nuclei. In particular, photon tagging can be used to measure Compton scattering on weakly-bound systems, since it facilitates the separation of elastic and inelastic cross sections. At sufficiently low incoming (outgoing) photon energy ω (ω') and momentum \vec{k} (\vec{k}'), the spin-averaged Compton scattering amplitude for any nucleus is, in the nuclear rest frame:

$$T = \vec{\epsilon}' \cdot \vec{\epsilon} \left(-\frac{Z^2 e^2}{m_A} + 4\pi\alpha\omega\omega' \right) + 4\pi\beta \vec{\epsilon}' \times \vec{k}' \cdot \vec{\epsilon} \times \vec{k} + \dots, \quad (1)$$

where $\vec{\epsilon}$ and $\vec{\epsilon}'$ are the polarization vectors of the initial and final-state photons. The first term in this series is a consequence of gauge invariance, and is the Thomson limit for low-energy scattering on a target of mass m_A

and charge Ze . The coefficients of the second and third terms are the target electric and magnetic polarizabilities, α and β , respectively. The polarizabilities can be separated by the angular dependence: for example, at forward (backward) angles the amplitude depends only on $\alpha + \beta$ ($\alpha - \beta$). Other terms, represented by “...”, include higher powers of energy and momentum.

Hydrogen targets are used to determine proton polarizabilities α_p and β_p [2]. By contrast, the absence of dense, stable, free neutron targets requires that the neutron polarizabilities α_n and β_n be extracted from scattering on deuterium (or other nuclear) targets. Data exist for coherent $\gamma d \rightarrow \gamma d$ from 49 to 95 MeV [3, 4, 5], and for quasi-free $\gamma d \rightarrow \gamma pn$ from 200 to 400 MeV [6]. The coherent process is sensitive to the isoscalar nucleon polarizabilities— $\alpha_N \equiv (\alpha_p + \alpha_n)/2$, $\beta_N \equiv (\beta_p + \beta_n)/2$ —via interference with the larger Thomson term. The extraction of these polarizabilities from data requires a consistent theoretical framework that clearly separates nucleon properties from nuclear effects. In the long-wavelength limit pertinent to polarizabilities EFT provides a model-independent way to do exactly this [7, 8, 9].

The EFT of QCD relevant to the low-energy interactions of a single nucleon with any number of pions and photons is known as chiral perturbation theory (χ PT). Many processes have been computed in this EFT to non-trivial orders and it has proven remarkably successful [8]. In this, as in any EFT, detailed information about short-distance physics is absent. The short-distance physics relevant to low-energy processes appears in the theory as constants whose determination lies outside the purview of the EFT itself. In the purest form of the theory they are determined by fitting experimental observables. In many cases the sparsity of low-energy single-nucleon data makes such a determination problematic—and for free neutrons data is non-existent.

At energies well below the chiral symmetry breaking scale, $\Lambda_\chi \sim 4\pi f_\pi \sim m_N \sim m_\rho$, an EFT of QCD can be built from the most general Lagrangian involving pions, nucleons and delta isobars, constrained only by ap-

proximate chiral symmetry and the relevant space-time symmetries. S -matrix elements can be expressed as a simultaneous expansion in powers of momenta and the pion mass over the characteristic scale of physics not included explicitly in the EFT. Thus, a generic amplitude may be written:

$$T = C(\Lambda_\chi) \sum_\nu \left(\frac{Q}{\Lambda_\chi} \right)^\nu \mathcal{F}_\nu(Q/m_\pi), \quad (2)$$

where Q represents the typical external momentum, \mathcal{F}_ν are calculable functions with $\mathcal{F}_\nu(1) = \mathcal{O}(1)$, C is an overall normalization factor, and ν is a counting index.

For energies comparable to the pion mass, the delta isobars can be integrated out of the EFT. When $\mathcal{F}_\nu(Q/m_\pi)$ in Eq. (2) for unpolarized Compton scattering is expanded in powers of Q , we obtain Eq. (1) with α and β given as functions of the EFT parameters. To $\mathcal{O}(Q^3)$, no parameters appear apart from those fit in other processes, so predictions can be made. At this order the proton and neutron polarizabilities are given by pion-loop effects [10]: $\alpha_p = \alpha_n = 10\beta_p = 10\beta_n = 5e^2g_A^2/384\pi^2f_\pi^2m_\pi = 12.2 \times 10^{-4} \text{ fm}^3$. Here $g_A \simeq 1.26$ is the axial coupling of the nucleon and $f_\pi \simeq 93 \text{ MeV}$ is the pion decay constant. At $\mathcal{O}(Q^4)$ there are new long-range contributions to these polarizabilities. Four new parameters also appear which encode contributions of short-distance physics. Thus, minimally, one needs four pieces of experimental data to fix these four short-distance contributions, but once they are fixed χ PT makes model-independent predictions for Compton scattering on protons and neutrons.

The amplitude for Compton scattering on the nucleon has been computed to $\mathcal{O}(Q^4)$ in Ref. [11]. The shifts of α_p and β_p from their $\mathcal{O}(Q^3)$ values were not fitted directly to the data in that work. Instead the Particle Data Group values for the polarizabilities were used [12]. These were originally extracted using a dispersion-theoretic approach that incorporates model-motivated assumptions regarding the asymptotic behavior of the amplitude. The differential cross sections which result from this procedure are in good agreement with the low-energy data [2].

Thus the calculation of Ref. [11] is not, strictly speaking, model independent: there is model input in the values used for α_p and β_p . If one insists on model-independence, very good fits of the proton data in the low-energy regime ($\omega, \sqrt{|t|} < 200 \text{ MeV}$) can be obtained. The central values for α_p and β_p are similar to those employed in Ref. [11], but the uncertainty is larger:

$$\begin{aligned} \alpha_p &= (12.1 \pm 1.1)^{+0.5}_{-0.5} \times 10^{-4} \text{ fm}^3, \\ \beta_p &= (3.4 \pm 1.1)^{+0.1}_{-0.1} \times 10^{-4} \text{ fm}^3, \end{aligned} \quad (3)$$

where statistical errors are inside the brackets, and an estimate of the contribution from higher-order terms is given outside. These numbers are based on varying the upper bound on which data are fit from 160 MeV to 200 MeV, and on estimates of the $\mathcal{O}(Q^5)$ effect on γp scat-

tering. A sample of the best-fit results is shown, together with data, in Fig. 1. The fit has $\chi^2/\text{d.o.f.} = 170/131$.

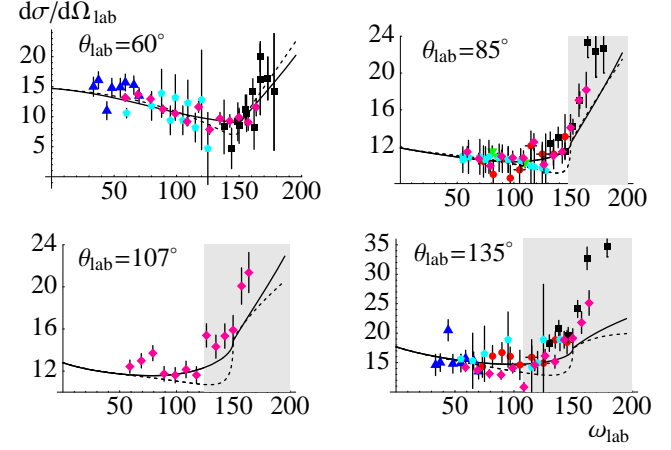


FIG. 1: Results of the $\mathcal{O}(Q^4)$ EFT best fit (solid line) to the differential cross sections for Compton scattering on the proton at four different angles, compared to the experimental data [2]. (Symbols as in Ref. [11].) The grey area is the region excluded from the fit ($\omega, \sqrt{|t|} > 200 \text{ MeV}$). The dashed line is the $\mathcal{O}(Q^3)$ prediction.

The amplitude for Compton scattering on a nuclear target can also be calculated in the EFT, although the unraveling of scales is more subtle when more than one nucleon is present [9]. In the single-nucleon sector a typical intermediate state has an energy denominator of $\mathcal{O}(Q)$, but in multi-nucleon processes “reducible” intermediate states can have small energy denominators of $\mathcal{O}(Q^2/m_N)$. The resulting infrared enhancement complicates the perturbative expansion [13]. Furthermore, the very existence of nuclei implies a breakdown of perturbation theory; hence the leading two-nucleon interactions should be summed to all orders, thereby building up a nuclear wave function $|\psi\rangle$. In the case of Compton scattering at energies of $\mathcal{O}(m_\pi)$, this is the only resummation necessary [14], and the full amplitude, T , can be written in terms of a kernel $K_{\gamma\gamma}$ which contains all irreducible (in the above sense) $\gamma NN \rightarrow \gamma NN$ graphs:

$$T = \langle \psi | K_{\gamma\gamma} | \psi \rangle. \quad (4)$$

The kernel can be calculated in χ PT. Several other reactions involving deuterium have been successfully analyzed using analogous approaches [9]. However, for Compton scattering at energies of $\mathcal{O}(m_\pi^2/m_N)$ further resummations are necessary. In particular, such resummations restore the Thomson limit for Compton scattering from deuterium [14, 15, 16]. In this energy regime it seems more appropriate to use a lower-energy EFT where pions have been integrated out [17].

At momentum transfers of $\mathcal{O}(m_\pi)$, a formally-consistent power counting is emerging [18] which organizes the nuclear interactions that give rise to the wave function $|\psi\rangle$. This power counting is an improvement

Chiral order	Wave function	Very-low-energy resummation?	$\omega, \sqrt{ t }$	$\alpha_N(10^{-4} \text{ fm}^3)$	$\beta_N(10^{-4} \text{ fm}^3)$	$\chi^2/\text{d.o.f.}$
Q^4	NLO χ PT	No	< 160 MeV	11.1	1.3	2.32
Q^4	NLO χ PT	Yes	< 160 MeV	9.0	1.7	1.48
Q^4	NLO χ PT	Yes	< 200 MeV	8.2	3.1	1.58
Q^4	Nijm93	Yes	< 160 MeV	12.6	1.1	2.95

TABLE I: Results from different χ PT extractions of isoscalar nucleon polarizabilities from γd scattering data.

over Weinberg’s original proposal [13], which has led to fairly accurate wave functions [9]. To the order we are working in the EFT, we require a deuteron wave function calculated to $\mathcal{O}(Q^2)$ in the chiral expansion. We employ a wave function generated using the $\mathcal{O}(Q^2)$ χ PT potential of Ref. [19]. (The $\Lambda = 600$ MeV wave function was chosen, but choosing $\Lambda = 540$ MeV instead produces very similar results.) In order to test the consistency of our error estimates, we have also computed results with other “realistic” wave functions, such as that obtained from the Nijm93 OBE potential [20].

Meanwhile, the kernel $K_{\gamma\gamma}$ is the sum of the single-nucleon Compton amplitude, in which one nucleon is a “spectator” to the Compton scattering, and “two-nucleon” contributions in which both nucleons are involved in the scattering of the photon. The amplitude for coherent Compton scattering on the deuteron was computed to $\mathcal{O}(Q^3)$ in Ref. [14]. There are no free parameters to this order. The corresponding cross section is in good agreement with the Illinois data [3] at 49 and 69 MeV, but underpredicts the SAL data [4] at 95 MeV. This calculation yields cross sections which agree well with the recent Lund data [5]. It also agrees qualitatively with potential-model calculations of γd scattering [21, 22].

We have now extended our calculation to $\mathcal{O}(Q^4)$. The single-nucleon amplitude from Ref. [11] is boosted to the appropriate frame so as to account for “Fermi motion”, and the two-nucleon diagrams at $\mathcal{O}(Q^4)$ are added to the two-nucleon $\mathcal{O}(Q^3)$ diagrams shown in Ref. [14]. These $\mathcal{O}(Q^3)$ graphs were generated by the leading chiral Lagrangian. In going to $\mathcal{O}(Q^4)$ we include diagrams with one insertion from the sub-leading chiral Lagrangian. The coefficients of these vertices are essentially determined by relativistic invariance, and so these $\mathcal{O}(Q^4)$ two-body effects are suppressed by Q/m_N . No unknown parameters occur in these graphs. However, two free parameters do appear in the single-nucleon contribution: the shifts in the isoscalar polarizabilities from their $\mathcal{O}(Q^3)$ values. Indeed, of all the additional graphs which enter our new, $\mathcal{O}(Q^4)$, calculation only this effect from single-nucleon Compton scattering changes the cross section significantly. (Details can be found in Ref. [23].)

We have fitted these two free parameters to the existing γd scattering data. As in the proton case, we impose a cutoff on the data that we fit when we extract α and β . With a cutoff of $\omega, \sqrt{|t|} < 200$ MeV all of the 29 world data points [3, 4, 5] are included. We also use a cutoff of 160 MeV, in which case all but the two

backward-angle SAL points must be fitted. In both cases we float the experimental normalization for each experimental run within the quoted systematic error [24], resulting in 22 (20) degrees of freedom for the fit [23].

Using the wave function of Ref. [19], we fit to data with $\omega, \sqrt{|t|} < 160$ MeV. This produces the isoscalar nucleon polarizabilities and the χ^2 per degree of freedom given in the first line of Table I. The χ^2 is unacceptably large. This is driven mainly by the 49 MeV data from Illinois, and occurs because, as discussed above, for $\omega \sim m_\pi^2/m_N$ further resummations are necessary in the EFT. Here we adopt the strategy of including the dominant contributions that need to be added to our standard $\mathcal{O}(Q^4)$ result in this very-low-energy region in order to restore the Thomson limit for the γd amplitude [14]. This yields the results on the second line of Table I. An alternative strategy, namely dropping the 49 MeV data altogether, produces very similar central values for α_N and β_N .

When the upper limit on which data is fitted is increased the central value of $\alpha_N - \beta_N$ changes markedly, with the χ^2 per degree of freedom slightly higher (third line of Table I). Another key test involves examining the impact of the choice of deuteron wave function. The variability in the differential cross section due to the choice of wave function is $\sim 10\%$. When the Nijm93 wave function is used the results are as shown in the fourth line of Table I. The high χ^2 is again due to a failure to reproduce the 49 MeV data—this time even with the very-low-energy contributions included. While the Nijm93 wave function is not consistent with χ PT, it does have the correct long-distance behavior. Such sensitivity to the choice of $|\psi\rangle$ is worrisome and merits further study.

Putting these results together we conclude that our best fit, and error bars, for the *isoscalar nucleon* polarizabilities are:

$$\begin{aligned} \alpha_N &= (9.0 \pm 1.5)^{+3.6}_{-0.8} \times 10^{-4} \text{ fm}^3, \\ \beta_N &= (1.7 \pm 1.5)^{+1.4}_{-0.6} \times 10^{-4} \text{ fm}^3. \end{aligned} \quad (5)$$

The errors inside the brackets are statistical, and those outside reflect the arbitrariness as to which data are included, and different choices for $|\psi\rangle$. The results for the best-fit EFT are shown in Fig. 2.

Adding statistical errors in quadrature and including the theory errors linearly we infer values of α_n ranging from 0.6 to 16.8 (10^{-4} fm^3) and β_n between -4.5 and 6.1 (same units). Therefore, a wide range of neutron polarizabilities is consistent with a model-independent

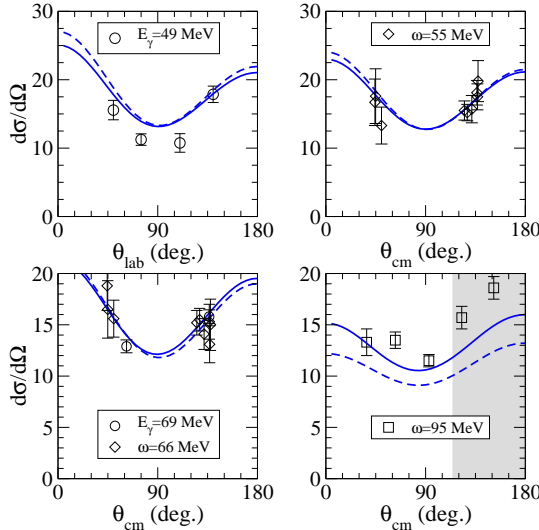


FIG. 2: Results of the $\mathcal{O}(Q^4)$ EFT best fit to the (lab. and c.m. as appropriate) differential cross sections for Compton scattering on deuterium at four different photon energies: 49 MeV lab. and 55, 66, and 95 MeV c.m. The data are from Illinois [3] (circles), Lund [5] (diamonds) and SAL (squares) [4]. The solid line is the $\mathcal{O}(Q^4)$ calculation with $\alpha_N = 9.0 \times 10^{-4} \text{ fm}^3$, $\beta_N = 1.7 \times 10^{-4} \text{ fm}^3$. The grey area is the region excluded from the fit ($\omega, \sqrt{|t|} > 160 \text{ MeV}$). The dashed line is the (parameter-free) $\mathcal{O}(Q^3)$ calculation.

analysis of the current low-energy γd and γp data. Narrower ranges can be obtained at the expense of introducing model dependence.

In conclusion, we have determined nucleon polarizabil-

ities from a model-independent fit to low-energy Compton scattering on the proton and the deuteron. Our results are consistent, within error bars, with the recent extraction of $\alpha_N \pm \beta_N$ from the Lund data using the detailed model of Levchuk and L'vov [5, 22]. (But see also the values found using the data of Refs. [3, 4] and this model [4, 22].). They are also consistent with the Baldin sum rule results for $\alpha_p + \beta_p$ and $\alpha_n + \beta_n$ [25]. The EFT can be improved by the introduction of an explicit Δ -isobar field, a complete treatment of the very-low-energy region, and a better understanding of the dependence of the results on the choice of deuteron wave function. An EFT study of the quasi-free deuteron process is also an important future step.

Acknowledgments

Discussions with T. Hemmert are gratefully acknowledged. We also thank E. Epelbaum and V. Stoks for providing us with deuteron wave functions, M. Lucas for discussions regarding data, and J. Brower for coding assistance. MM, DP, and UvK thank the Nuclear Theory Group at the University of Washington for hospitality while part of this work was carried out, and UvK thanks RIKEN, Brookhaven National Laboratory and the U. S. DOE [DE-AC02-98CH10886] for providing the facilities essential for the completion of this work. This research is supported in part by the US DOE under grants DE-FG03-97ER41014 (SRB), DE-FG02-93ER40756 (DRP), by the UK EPSRC (JM), by Brazil's CNPq (MM), by DOE OJI Awards (DP, UvK) and by an Alfred P. Sloan Fellowship (UvK).

-
- [1] B.R. Holstein, Comm. Nucl. Part. Phys. **20**, 301 (1992).
[2] P.S. Baranov *et al.*, Sov. J. Nucl. Phys. **21**, 355 (1975); F.J. Federspiel *et al.*, Phys. Rev. Lett. **67**, 1511 (1991); A. Ziegler *et al.*, Phys. Lett. B **278**, 34 (1992); E.L. Hallin *et al.*, Phys. Rev. C **48**, 1497 (1993); B.E. MacGibbon *et al.*, Phys. Rev. C **52**, 2097 (1995); V. Olmos de León *et al.*, Eur. Phys. J. A **10**, 207 (2001).
[3] M. Lucas, Ph.D. thesis, University of Illinois, unpublished (1994).
[4] D.L. Hornidge *et al.*, Phys. Rev. Lett. **84**, 2334 (2000).
[5] M. Lundin *et al.*, nucl-ex/0204014.
[6] N.R. Kolb *et al.*, Phys. Rev. Lett. **85**, 1388 (2000); K. Kossert *et al.*, nucl-ex/0201015.
[7] D.B. Kaplan, nucl-th/9506035; D.R. Phillips, Czech J. Phys. **52**, B49 (2002).
[8] V. Bernard, N. Kaiser, and U.-G. Meißner, Int. J. Mod. Phys. **E4**, 193 (1995).
[9] P.F. Bedaque and U. van Kolck, nucl-th/0203055; S.R. Beane, P.F. Bedaque, W.C. Haxton, D.R. Phillips, and M.J. Savage, Encyclopedia of Analytic QCD, At the Frontier of Particle Physics, vol. 1, 133-269, edited by M. Shifman (World Scientific).
[10] V. Bernard, N. Kaiser, and U.-G. Meißner, Nucl. Phys. **B383**, 442 (1992); V. Bernard, N. Kaiser, J. Kambor, and U.-G. Meißner, Nucl. Phys. **B388**, 315 (1992).
[11] J.A. McGovern, Phys. Rev. C **63**, 064608 (2001), see also nucl-th/0101057 v2.
[12] D.E. Groom *et al.* [Particle Data Group], Eur. Phys. J. C **15**, 1 (2000).
[13] S. Weinberg, Phys. Lett. B **251**, 288 (1990); Nucl. Phys. B **363**, 3 (1991).
[14] S.R. Beane, M. Malheiro, D.R. Phillips, and U. van Kolck, Nucl. Phys. A **656**, 367 (1999); M. Malheiro, S.R. Beane, D.R. Phillips, and U. van Kolck, nucl-th/0111047.
[15] J.L. Friar and E.I. Tomusiak, Phys. Lett. B **122**, 11 (1983).
[16] J.W. Chen, H.W. Grießhammer, M.J. Savage, and R.P. Springer, Nucl. Phys. A **644**, 245 (1998).
[17] S.R. Beane and M.J. Savage, Nucl. Phys. A **694** 511 (2001); H.W. Grießhammer and G. Rupak, Phys. Lett. B **529**, 57 (2002).
[18] S.R. Beane, P.F. Bedaque, M.J. Savage, and U. van Kolck, Nucl. Phys. A **700**, 377 (2002).

- [19] E. Epelbaum, W. Glöckle, and U.-G. Meißner, Nucl. Phys. A **671**, 295 (2000).
- [20] V.G. Stoks, R.A. Klomp, C.P. Terheggen and J.J. de Swart, Phys. Rev. C **49**, 2950 (1994). Our kernel is derived for low momenta, so we have applied an integration cutoff of 600 MeV when this wave function is used, so we can make a consistent comparison with our other results.
- [21] T. Wilbois, P. Wilhelm, and H. Arenhövel, Few-Body Syst. Suppl. **9**, 263 (1995); J.J. Karakowski and G.A. Miller, Phys. Rev. C **60**, 014001 (1999).
- [22] M.I. Levchuk and A.I. L'vov, Nucl. Phys. **A674**, 449 (2000).
- [23] S.R. Beane, M. Malheiro, J.A. McGovern, D.R. Phillips, and U. van Kolck, in preparation.
- [24] P.S. Baranov, A.I. L'vov, V.A. Petrun'kin, and L.N. Shtarkov, Phys. Part. Nucl. **32**, 376 (2001).
- [25] D. Babusci, G. Giordano, and G. Matone, Phys. Rev. C **57**, 291 (1998).